EFFECT OF NITRIDING PARAMETER ON ACTIVE SCREEN PLASMA NITRIDING RESPONSE OF SACM645 STEEL

Akio NISHIMOTO[1*], Hiroaki NII[2], Takumi HARUNA[1], Toru MARUYAMA[1] and Hidekazu MIYAKE[1]

(Received October 20, 2011)

Abstract

A nitriding steel SACM645 was active screen plasma nitrided using an austenitic stainless-steel screen to investigate the effect of nitriding parameters such as gas pressure and the distance between the screen and the sample on the nitriding response. The sample was treated for 18 ks at 823 K in 25% N_2 + 75% H_2. The gas pressure was changed to 100, 600, and 1200 Pa. The distance between the screen and the sample was also changed to 10, 30, and 50 mm. The nitrided samples were characterized by observing their surface morphology and cross-sectional microstructure by scanning electron microscopy, X-ray diffraction, and microhardness testing. After nitriding, polygonal particles with a normal distribution were observed at the center and edges of all nitrided sample surfaces. The particles on the sample surface became finer with an increase in the gas pressure. A nitrided layer with a greater and homogeneous thickness was obtained at a low gas pressure of 100 Pa.

1. Introduction

The nitriding process is widely used to improve the tribological properties and wear resistance of steels and titanium alloys. Compared with the conventional nitriding processes such as gas nitriding and salt bath nitriding, the glow-discharge plasma nitriding process offers the following advantages: no pollution, high nitrogen potential, short treatment time, clean environment, and low energy consumption[1-3]. The components to be treated are subjected to a high cathodic potential to produce plasma directly on their surfaces. An "edging effect" occurs due to distortions in the electric field around the corners and edges of the components although the components are well heated. This results in nonuniformity in properties such as the hardness and thickness of the surface layer[4].

Recently, there has been considerable interest in active screen plasma nitriding (ASPN), through-cage plasma nitriding (TCPN), and cathodic-cage plasma nitriding (CCPN)[5-20]. In these processes, the edging effect is completely eliminated because the plasma is produced on the cage and not directly on the samples[5]. These processes can be used to treat polymers that are nonconductive materials[7, 11]. However, little has been reported on the effect of the gas pressure

[1] Department of Chemistry and Materials Engineering, Faculty of Chemistry, Materials and Bioengineering, Kansai University, Suita, Osaka 564-8680, Japan
[2] Graduate School of Science and Engineering, Kansai University, Suita, Osaka 564-8680, Japan
* Corresponding author: Akio Nishimoto, Department of Chemistry and Materials Engineering, Faculty of Chemistry, Materials and Bioengineering, Kansai University, Suita, Osaka 564-8680
E-mail: akionisi@kansai-u.ac.jp

and the distance between the screen and the sample on ASPN responses such as surface morphology, microstructure, and nitrogen depth[19, 20].

In this study, nitriding steel samples were nitrided by ASPN to investigate the effect of the nitriding parameters on ASPN responses.

2. Materials and Methods

The sample material used in this study was a nitriding steel SACM645 (chemical composition (mass%): 0.46% C, 1.57% Cr, 0.85% Al, 0.15% Mo, 0.54% Mn and balance Fe). The sample disk was 13 mm in diameter and 5 mm in thickness. The sample surface was mechanically ground with 150- to 1500-grit SiC, finely polished with 0.05-μm alumina in suspension, degreased ultrasonically in acetone, and dried in air before the sample was placed in the nitriding furnace.

ASPN experiments were carried out using a direct-current (DC) plasma-nitriding unit (NDK, Inc. Japan, JIN-1S). Figure 1 presents a schematic diagram of the ASPN apparatus. A quartz (SiO_2) rod was placed on the cathodic stage in order to construct an isolated sample stage. The sample was placed on the sample stage in a floating potential and isolated from the cathodic screen and the anode. The screen, which was an expanded metal mesh of austenitic stainless steel SUS304 with a diameter of 150 mm and a height of 155 mm, was mounted on the cathodic stage around the sample stage. Mesh specifications of the expanded metal mesh used were L × S of 8 × 3 mm and thickness of 0.5 mm. SUS304 rods were placed on the sample stage so that the distance between the screen and the sample could be changed to 10, 30, and 50 mm. The screen was thoroughly degreased ultrasonically in acetone.

Nitriding was performed in a nitrogen-hydrogen atmosphere with 25% N_2 + 75% H_2 for 18 ks at 823 K under 100, 600, and 1200 Pa by the ASPN process. After placing the sample on the sample stage, the chamber was evacuated at ~3 Pa. Then, nitrogen and hydrogen were introduced into the chamber, and a DC bias voltage was supplied. After nitriding, the DC supply was switched off, and the sample was cooled to room temperature in the furnace. The nitriding temperature was monitored using a radiation thermometer. The radiation thermometer was positioned at the sample in which the distance between the screen and the

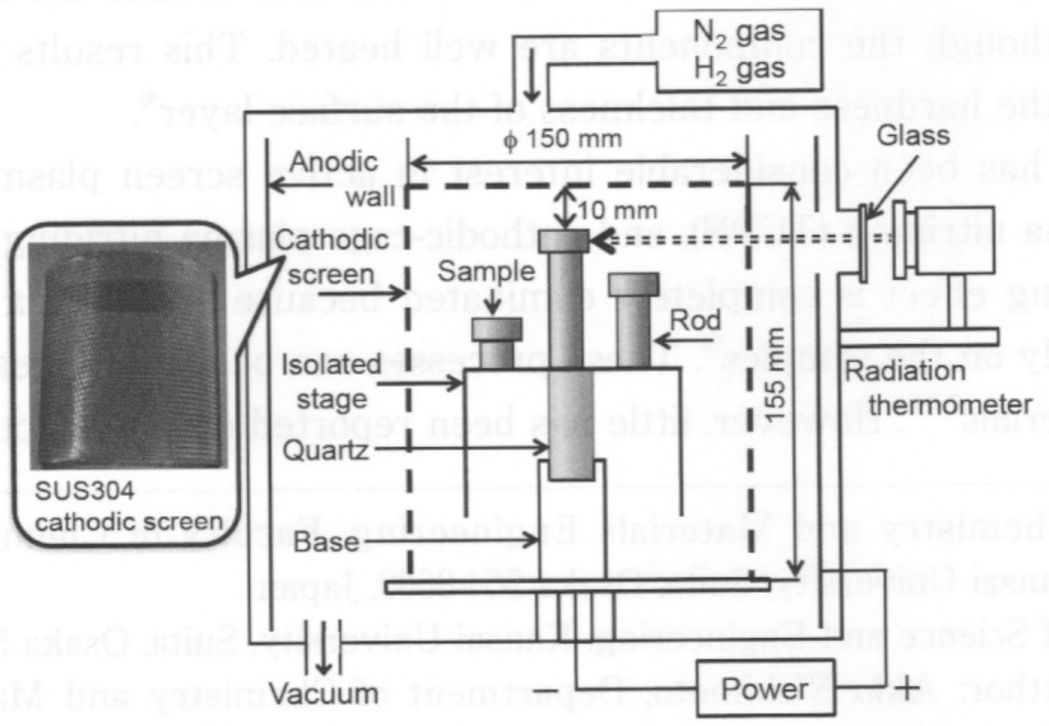

Fig. 1 Schematic illustration of ASPN furnace.

sample was 10 mm, as depicted in Fig. 1.

After nitriding, cross sections of each sample were first cut using a low-speed saw and then polished and chemically etched. The nitrided microstructure was examined using a scanning electron microscope (SEM; JEOL, Japan, JSM-6060LV). The phase structures on the nitrided surface were determined by theta-2theta X-ray diffraction (XRD, Rigaku, Japan, RINT-2550V) studies. The entire area of the top surface of nitrided samples was analyzed by XRD. In addition, the hardness of the surface and the cross sections of the nitrided sample were measured using a Vickers microhardness tester (Matsuzawa, Japan, MXT50) under a 0.1 N load. Five indentations were performed on each sample, and a 3-point average value (except both maximum and minimum values) was used for hardness.

3. Results and Discussion

After treatment, the appearances of the samples were examined visually (Fig. 2). The edging effect was not observed in the samples. This shows that glow discharge did not occur on the sample surface because the sample was isolated by placing SiO_2 ceramics between the sample and the cathodic stage. Furthermore, in the ASPN process, the samples were heated to the treatment temperature by the heat radiated from the active screen, which promoted a higher homogeneity of temperature in the treated samples[5].

XRD results of the samples treated by the ASPN process are shown in Fig. 3. α-ferrite, CrN and γ'-Fe_4N were identified on the sample surface under each condition. The layers formed on each sample were of the same phase, irrespective of the gas pressure and the distance between the screen and the sample.

Figure 4 presents SEM micrographs of the sample surfaces treated by the ASPN process. The surface morphologies of samples treated at different pressures are different. Under the same gas pressure, a uniform, normal distribution of polygonal particles was observed at the center and edges of the sample surface, irrespective of the distance between the screen and

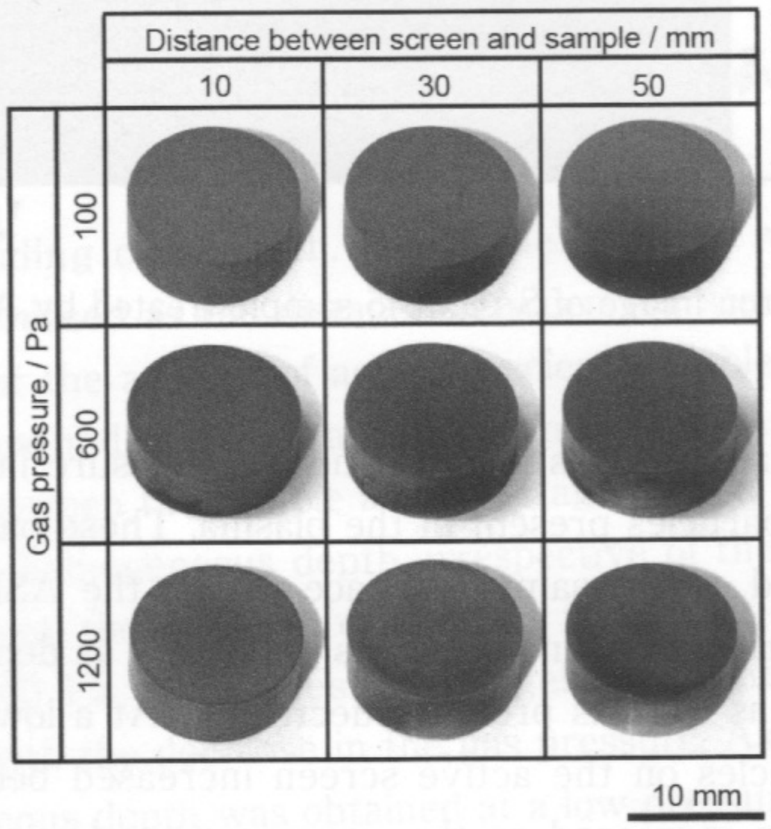

Fig. 2 Appearance of SACM645 sample treated by ASPN at 823 K for 18 ks.

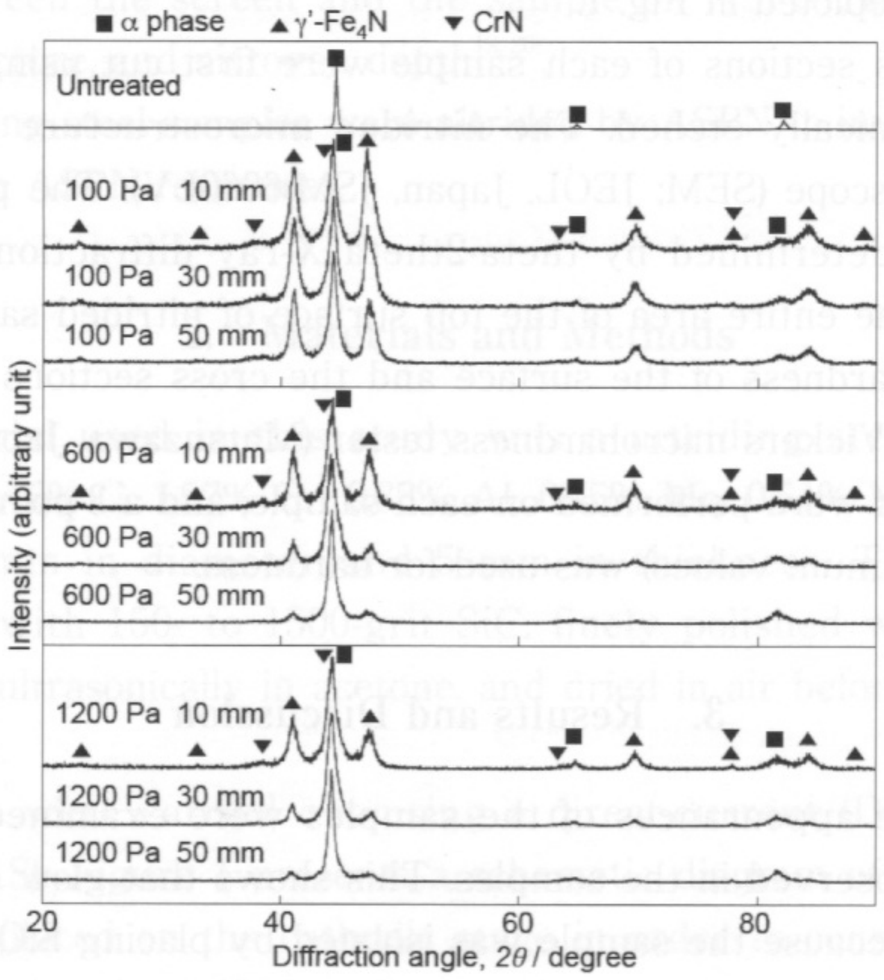

Fig. 3 XRD pattern of SACM645 sample treated by ASPN at 823 K for 18 ks.

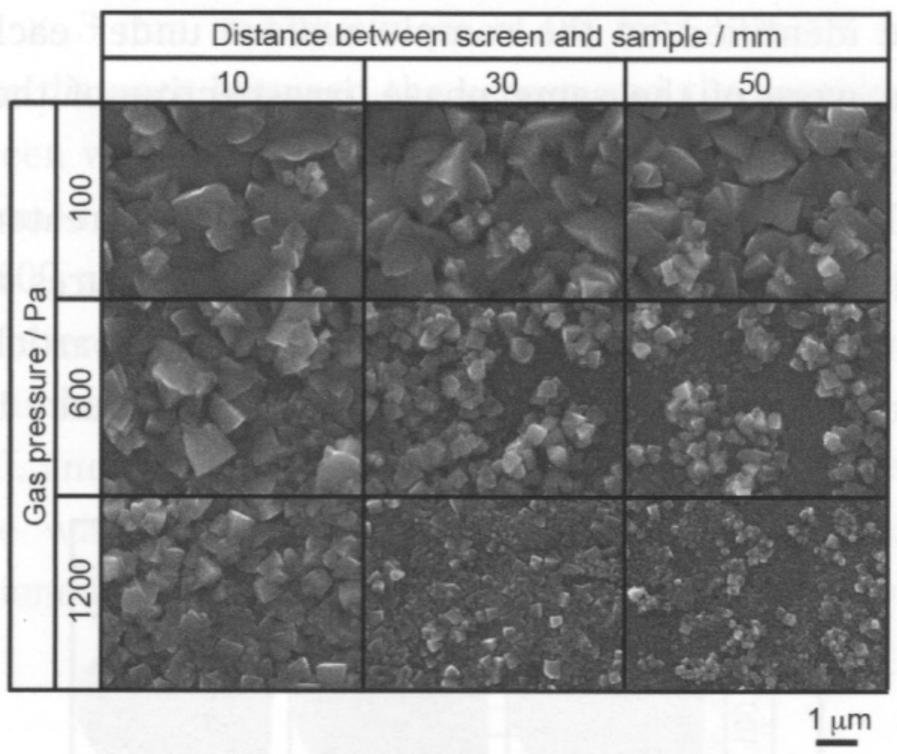

Fig. 4 Secondary electron image of SACM645 sample treated by ASPN at 823 K for 18 ks.

the sample. The particle size becomes finer as the gas pressure increases. These results can be attributed to the Fe_xN particles present in the plasma. These particles were formed on the active screen and deposited on the sample surface during the ASPN process. Moreover, the applied voltages during nitriding depended on gas pressures, as depicted in Fig. 5. That is, the applied voltages increased as the gas pressure decreased. At a lower pressure of 100 Pa, the number of sputtered particles on the active screen increased because of the high voltage. Therefore, Fe_xN deposition increased as the gas pressure decreased, and these deposited particles grew in number, as depicted in Fig. 6.

Figure 7 depicts the effect of the gas pressure and the distance between the screen and

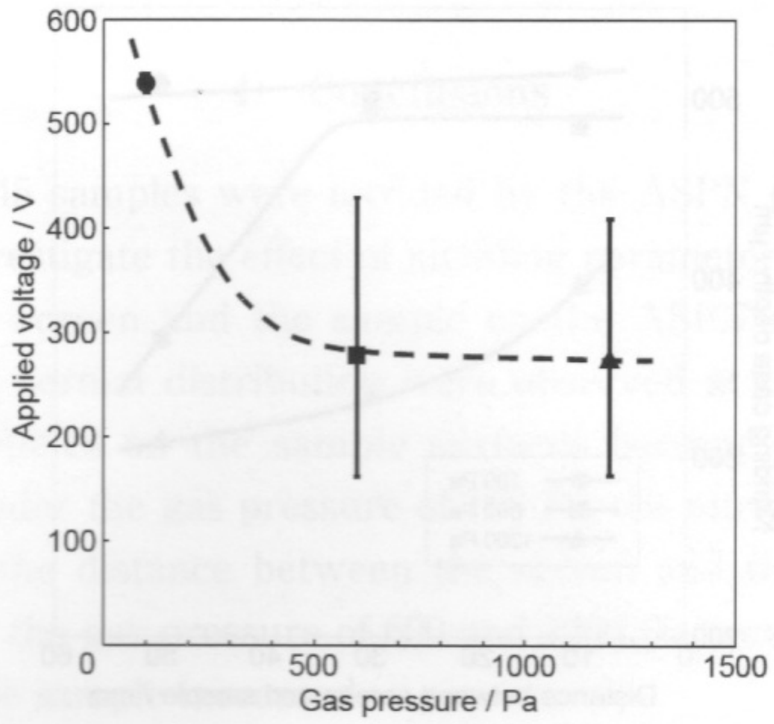

Fig. 5 Relationships between applied voltage and gas pressure of SACM645 sample treated by ASPN at 823 K for 18 ks.

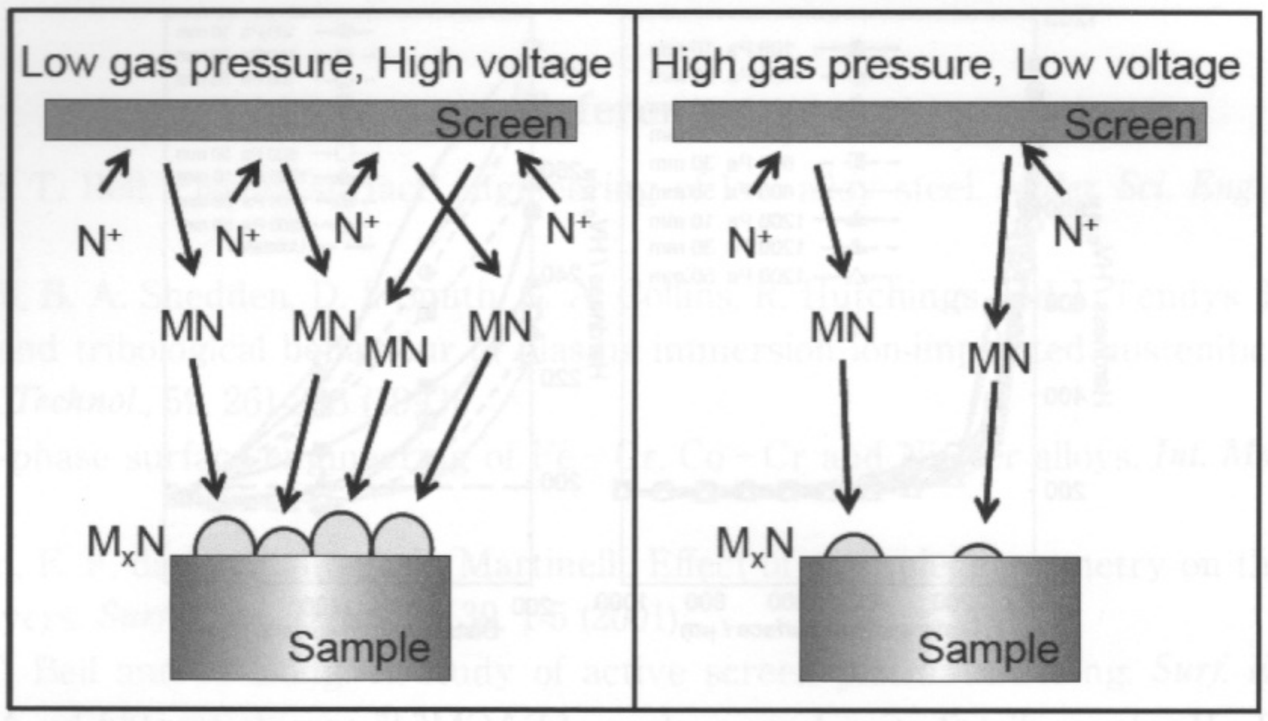

Fig. 6 Schematic illustration of mechanism of nitrogen mass transfer in ASPN.

the sample on the nitriding case depth. When the samples were treated at 1200 Pa, the nitriding case depth decreased as the distance between the screen and the sample increased. This result indicates that the amount of active species available for nitriding depends on the distance between the cathodic screen and the sample because the sample is isolated by placing SiO_2 ceramics between the sample and the stage. On the other hand, the nitrided layer treated at 100 Pa had a homogeneous depth, irrespective of the distance between the screen and the sample. Moreover, the nitriding case depth treated at 100 Pa was greater than that treated at 600 and 1200 Pa. These results suggest that the homogeneous temperature distribution expanded with the decrease in the gas pressure. As a result, a nitrided layer with a greater and homogeneous depth was obtained at a low pressure of 100 Pa.

Figure 8 shows the cross-sectional hardness distribution of the samples treated by the ASPN process. The hardness decreased considerably toward the core of the substrate,

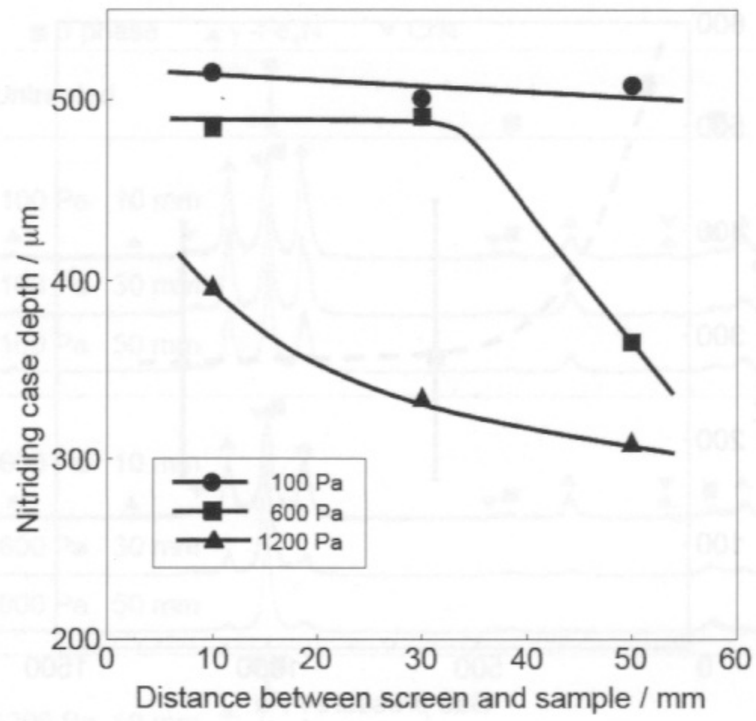

Fig. 7 Nitriding case depth of SACM645 sample treated by ASPN at 823 K for 18 ks.

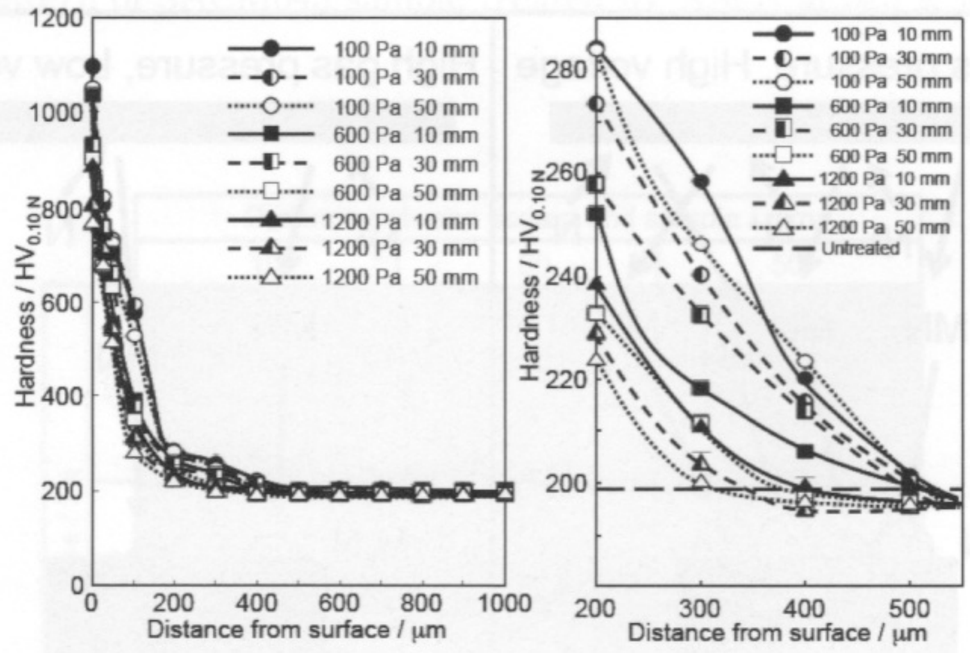

Fig. 8 Hardness distribution from surface of SACM645 sample treated by ASPN at 823 K for 18 ks. (a) from 0 to 1000 μm and (b) from 200 to 550 μm.

irrespective of the gas pressure and the distance between the screen and the sample. In addition, the hardening effect of the sample nitrided at 100 Pa was greater than that nitrided at 600 and 1200 Pa. The dependence of the distance on the surface hardness is a result of the nitriding case depth on the surface, as depicted in Fig. 7.

Alves Jr. *et al.* demonstrated that the nitriding case depth depends on the sample geometry during conventional DC plasma nitriding[4]. Jeong and Kim demonstrated that the nitriding case depth and particle size on the surface increased with increasing gas pressure for the DC plasma nitriding[21]. In the present investigation, the nitrided layer treated at a lower pressure of 100 Pa had a homogeneous thickness, irrespective of the distance between the screen and the sample and the sample geometry. Moreover, the nitriding case depth treated at 100 Pa was greater than that treated at 600 and 1200 Pa.

4. Conclusions

Nitriding steel SACM645 samples were nitrided by the ASPN process using an austenitic stainless-steel screen to investigate the effect of nitriding parameters such as gas pressure and the distance between the screen and the sample on the ASPN responses. After nitriding, polygonal particles with a normal distribution were observed at the center and edges of all sample surfaces. The particles on the sample surfaces became finer as the gas pressure increased. Furthermore, under the gas pressure of 100 Pa, the nitriding case depth was almost the same, irrespective of the distance between the screen and the sample. In contrast, the nitriding case depth under the gas pressure of 600 and 1200 Pa became smaller as the distance between the screen and the sample increased.

Acknowledgments

This research was financially supported by a Kansai University Grant-in-Aid for progress of research in graduate course, 2009.

References

1) Y. Sun and T. Bell. Plasma surface engineering of low alloy steel. *Mater. Sci. Eng. A*, 140, 419-434 (1991).
2) M. Samandi, B. A. Shedden, D. I. Smith, G. A. Collins, R. Hutchings and J. Tendys. Microstructure, corrosion and tribological behaviour of plasma immersion ion-implanted austenitic stainless steel. *Surf. Coat. Technol.*, 59, 261-266 (1993).
3) H. Dong. S-phase surface engineering of Fe－Cr, Co－Cr and Ni－Cr alloys. *Int. Mater. Rev.*, 55, 65-98 (2010).
4) C. Alves Jr., E. F. da Silva and A. E. Martinelli. Effect of workpiece geometry on the uniformity of nitrided layers. *Surf. Coat. Technol.*, 139, 1-5 (2001).
5) C. X. Li, T. Bell and H. Dong. A study of active screen plasma nitriding. *Surf. Eng.*, 18, 174-181 (2002).
6) C. X. Li and T. Bell. Corrosion properties of active screen plasma nitrided 316 austenitic stainless steel. *Corros. Sci.*, 46, 1527-1547 (2004).
7) C. X. Li and T. Bell. Potential of plasma nitriding of polymer for improved hardness and wear resistance. *J. Mater. Process. Technol.*, 168, 219-224 (2005).
8) P. Hubbard, S. J. Dowey, E. D. Doyle and D. G. McCulloch. Influence of bias and *in situ* cleaning on through cage (TC) or active screen plasma nitrided (ASPN) steels. *Surf. Eng.*, 22, 243-247 (2006).
9) C. Zhao, C. X. Li, H. Dong and T. Bell. Study on the active screen plasma nitriding and its nitriding mechanism. *Surf. Coat. Technol.*, 201, 2320-2325 (2006).
10) C. Alves Jr., F. O. de Araujo, K. J. B. Ribeiro, J. A. P. da Costa, R. R. M. Sousa and R. S. de Sousa. Use of cathodic cage in plasma nitriding. *Surf. Coat. Technol.*, 201, 2450-2454 (2006).
11) A. P. Kauling, G. V. Soares, C. A. Figueroa, R. V. B. de Oliveira, I. J. R. Baumvol, C. Giacomelli and L. Miotti. Polypropylene surface modification by active screen plasma nitriding. *Mater. Sci. Eng. C*, 29, 363-366 (2009).
12) A. Nishimoto, A. Tokuda and K. Akamatsu. Effect of through cage on active screen plasma nitriding properties. *Mater. Trans.*, 50, 1169-1173 (2009).
13) S. C. Gallo and H. Dong. Study of active screen plasma processing conditions for carburising and nitriding austenitic stainless steel. *Surf. Coat. Technol.*, 203, 3669-3675 (2009).

14) A. Nishimoto, T. E. Bell and T. Bell. Feasibility study of active screen plasma nitriding of titanium alloy. *Surf. Eng.*, 26, 74-79 (2010).
15) C. X. Li. Active screen plasma nitriding - an overview. *Surf. Eng.*, 26, 135-141 (2010).
16) P. Hubbard, J. G. Partridge, E. D. Doyle, D. G. McCulloch, M. B. Taylor and S. J. Dowey. Investigation of nitrogen mass transfer within an industrial plasma nitriding system I: the role of surface deposits. *Surf. Coat. Technol.*, 204, 1145-1150 (2010).
17) Y. Li, L. Wang, D. Zhang and L. Shen. Influence of bias voltage on the formation and properties of iron-based nitrides produced by plasma nitriding. *J. Alloys Compds.*, 497, 285-289 (2010).
18) Y. Dong, X. Li, R. Sammons and H. Dong. The generation of wear-resistant antimicrobial stainless steel surfaces by active screen plasma alloying with N and nanocrystalline. *J. Biomed. Mater. Res. Part B: Appl. Biomater.*, 93B, 185-193 (2010).
19) A. Nishimoto, K. Nagatsuka, R. Narita, H. Nii and K. Akamatsu. Effect of the distance between screen and sample on active screen plasma nitriding properties. *Surf. Coat. Technol.*, 205, S365-S368 (2010).
20) A. Nishimoto, K. Nagatsuka, R. Narita, H. Nii and K. Akamatsu. Effect of gas pressure on active screen plasma nitriding response. *J. ASTM Int.*, 8, JAI103286 (2011).
21) B. Y. Jeong and M. H. Kim. Effects of the process parameters on the layer formation behavior of plasma nitrided steels. *Surf. Coat. Technol.*, 141, 182-186 (2001).